Hindawi
Advances in Civil Engineering
Volume 2022, Article ID 1369171, 12 pages
https://doi.org/10.1155/2022/1369171

Research Article

Laboratory Tests on Open-Close Pile Jacking and Load Bearing Characteristics in Saturated Clay Soil

Qiang Song,[1] Teng Zhang,[2,3] Guangyu Zhou,[4] Hongzhong Li,[5] Xianghou Li,[6] Yishun Jiang,[6] Peng Zhao,[6] Weihui Tian,[7] Yonghong Wang,[2,8] Chuantong Zhang,[9] and Huining Liu[10]

[1]*Qingdao Vocational and Technical College of Hotel Management, Qingdao 266100, China*
[2]*School of Civil Engineering, Qingdao University of Technology, Qingdao 266033, China*
[3]*Qingdao Green Technology Geotechnical Engineering Co., Ltd., Qingdao 266033, China*
[4]*Department of Hydraulic Engineering, Shandong Water Conservancy Vocational College, Rizhao 276826, China*
[5]*Guangdong Province Communications Planning & Design Institute Co., Ltd., Guangzhou, China*
[6]*Shandong Luqiao Group Co., Ltd., Jinan, China*
[7]*Powerchina Northwest Engineering Corporation Limited, Xian, China*
[8]*Cooperative Innovation Center of Engineering Construction and Safety in Shandong Blue Economic Zone, Qingdao 266033, China*
[9]*China State Construction Zhongxin Construction Engineering Co., Ltd., Shandong Branch, Qingdao, China*
[10]*Shandong Hi-Speed Engineering Construction Group Co. Ltd., Jinan, China*

Correspondence should be addressed to Yonghong Wang; hong7986@163.com

Received 25 February 2022; Accepted 17 May 2022; Published 15 June 2022

Academic Editor: Angelo Aloisio

The stress characteristics of the pile-soil interface have an important influence on the effect and long-term bearing capacity of jacked piles. In order to obtain the stress characteristics of the pile-soil interface of the jacked pile in clay, the development law of pore water pressure and earth pressure for open- and closed-end jacked piles during the pile jacking process was studied using indoor model tests based on a saturated soft clay foundation. Test results show that, during the pile jacking process, the excess pore water pressure, earth pressure, and effective earth pressure at the pile-soil interface all increase gradually along penetration depth, and the increasing trend first increases linearly and then increases sharply at the pile end. The excess pore water pressure at the pile-soil interface of an open-end pile is smaller than that of a closed-end pile. The earth pressure and effective earth pressure at the pile-soil interface of the closed-end pile show a “lateral pressure degradation,” and the degradation becomes more and more significant with increasing depth. The pile-soil interface adhesion coefficient increases with increasing penetration depth, and the greater the adhesion coefficient is, the higher the tightness between the pile and soil will be. As a method of determining the interfacial tightness between the pile and soil, the adhesion coefficient is closely related to the excess pore water pressure and earth pressure generated during the pile jacking process and can accurately reflect the mechanical mechanism of pile jacking in saturated viscous soil. Results of this contribution can provide reference for theoretical research on the mechanical pile jacking mechanism in saturated viscous soil.

1. Introduction

Jacked piles are a significant component of many construction projects; hence, improving jacked pile technology is an urgent need [1–4]. The process of jacked pile sinking is considered to be static uniform speed penetration, and the pile side resistance is generated by the friction between the pile soil. Driven pile is sunk by the impact load of the pile hammer acting on the pile top, and the pile side resistance is generated under the action of the nonlinear pile soil with a large deformation of the dynamic height. However, many aspects of current jacked pile research are lacking [5–8]. Stress characteristics at the pile-soil interface have significant influence on the pile jacking process and long-term bearing capacity. The variation law of excess pore pressure and earth pressure caused by pile jacking is also significant [9, 10]. At present, scholars at home and abroad primarily use theoretical methods to study changes in earth pressure and pore water pressure caused by jacked pile penetration. Cao et al. [11] studied the pile side pressure, excess pore water pressure, and pile side soil displacement in the pile jacking process based on circular hole expansion theory and obtained the earth pressure, pore water pressure, and shallow soil displacement around the pile under various conditions. Tehrani et al. [12] further modified the theoretical solution for circular hole expansion theory on pile body resistance and pile-soil effect by considering the surface roughness and obtained the change rule of earth pressure in the radial direction and with depth. Burns and Mayne [13] obtained the variation law of pore water pressure in the pile jacking permeation in fine sand, silt, and soft soil and carried out function fitting in combination with the theory of circular hole expansion. Sagaseta [14] examined pore water pressure and earth pressure using the strain path method by considering the influence of depth change on soil displacement and continuity of the pile penetration process. Hoang et al. [15] investigated the pile installation effects on the behaviors of jacked in piles through three simulation techniques. Both the experimental results and calculated results using three techniques agreed well and indicated that ground consolidation caused by pile installation increases the pile bearing capacity and the pile shaft resistance. Xue et al. [16] studied the experimental tests of four RC pile specimens backfilled with different damping material to assess their effect on the soil-structure hysteretic response. Theoretical formulas are commonly unable to accurately apply the actual mechanical conditions of practical projects, so the distribution rules of excess pore water pressure and earth pressure around piles obtained by theoretical research methods are nongeneral and difficult to be popularized.

On the basis of field tests, some scholars have obtained the variation rules for the excess pore water pressure and earth pressure in the pile jacking process. Hwang et al. [17] found that the dynamic change of pore pressure was closely related to the pile penetration process by embedding sensors in the affected soil layer at a certain distance around the pile to observe the pore water pressure and earth pressure of the full-length pile during the pile jacking process. Cooke and Price [18] pushed a test pile into overconsolidated London clay and tested the pore water pressure of the soil around the pile after the jacking pile. Pestana et al. [19] compared and analyzed the dissipation law and influence range of the excess pore water pressure based on a large number of field tests and believed that measuring excess pore water pressure could effectively predict property changes in foundation soil. Doherty and Gavin [20], based on the field tests, discussed the pore water pressure in the pile jacking process, and the end condition has a certain influence on the pore water pressure. The excess pore water pressure and earth pressure caused by jacked pile construction obtained by field test have a guiding significance for pile foundation construction.

In the pile jacking process, excess pore water pressure and earth pressure at the pile-soil interface are different from excess pore water pressure and earth pressure in the soil within a given range around the pile. Lehane [21], based on field tests, found that soil pressure at the pile-soil interface at various positions decreased with increasing h/B (h is the distance between the sensor and the pile end; B is the pile diameter). Bond and Jardine [22] comprehensively and accurately tested the pore water pressure and effective radial stress at the pile-soil interface during the pile jacking process and under static loading. Kou et al. [23] studied the law of pore water pressure dissipation when the jacked pile penetrates into silt deposited soil based on field tests. Liu et al. [24] examined the performance of an open pile penetrating into a silty layer using an indoor model test and obtained the accumulation law for excess pore water pressure in the soil. Studying the changes in excess pore water pressure and earth pressure at the pile-soil interface caused by pile jacking in cohesive soil is of great significance.

Accurately measuring the interfacial earth pressure and pore water pressure caused by jacked pile penetration and determining the degree of bonding between piles and soil through the variation law of effective earth pressure at the pile-soil interface in the pile jacking process are the major difficulties in studying the pile jacking mechanism. In practical engineering applications, pile jacking is mostly used in clay soil. Clay soil can better reproduce the actual working state of pile jacking, so it is necessary to carry out a pile jacking penetration mechanism in clay soil foundations study [25, 26]. At present, there are relatively few studies on the stress characteristics at the pile-soil interface during the pile jacking process in viscous soil, especially comparative studies on open- and closed-end piles. Aiming at the plugging effect caused by the open pipe pile in the process of pile jacking, a more detailed experimental study of "soil plug resistance" in the separation of pile immersion resistance can be carried out [27]. Obtaining the variation law of excess pore pressure and earth pressure caused by pile jacking is urgent and necessary. This article is based on open- and closed-end model piles with sensors as well as pile jacking and static load laboratory tests in viscous soil. The variation law of excess pore water pressure and earth pressure at pile-soil interface generated in the pile jacking process and under static loading is obtained, and the concept expressed by the adhesion coefficient of the compaction degree between the pile-soil and earth pressure is determined. Results of this study can provide reference for theoretical research on mechanical pile jacking in saturated viscous soil.

2. Theoretical Calculation Method for Pore Water Pressure

Simulating the pile penetration process is a relatively complex problem in theory. At present, the data measured in field or indoor pile penetration processes indicate that most of the earth pressure and pore water pressure can be estimated using cylindrical hole expansion theory. For the saturated elastic and completely plastic material subject to the Mohr-Coulomb yield criterion, the total stress increment caused by expansion of the cylindrical hole [28] is

$$\begin{aligned}&\Delta\sigma_r = 2c_u \ln\left(\frac{R_p}{r}\right) + c_u,\\ \text{In the plastic zone } &\Delta\sigma_\theta = 2c_u \ln\left(\frac{R_p}{r}\right) - c_u,\\ &\Delta\sigma_z = 2c_u \ln\left(\frac{R_p}{r}\right),\end{aligned} \tag{1}$$

$$\begin{aligned}&\Delta\sigma_r = c_u \ln\left(\frac{R_p}{r}\right)^2,\\ \text{In the elastic zone } &\Delta\sigma_\theta = -c_u \ln\left(\frac{R_p}{r}\right)^2,\\ &\Delta\sigma_z = 0.\end{aligned} \tag{2}$$

$\Delta\sigma_r$, $\Delta\sigma_\theta$, and $\Delta\sigma_z$ are, respectively, the radial, tangential, and vertical stress increment; R is the distance from the pile center; R_p is the radius of plastic zone; C_u is the undrained soil shear strength.

The pore water pressure increment can be calculated according to the Henkel formula [29], as follows:

$$\Delta u = \beta\Delta\sigma_{\text{OCT}} + \alpha\Delta\tau_{\text{OCT}}, \tag{3}$$

where $\Delta\sigma_{\text{OCT}}$ and $\Delta\tau_{\text{OCT}}$ are the normal stress increment and shear stress increment of octahedron, respectively, β and α are Henkel pore water pressure parameters, and $\beta = 1$ for saturated soil.

The relationship between the Henkel pore water pressure parameter α and Skempton pore water pressure parameter A is as follows [30]:

$$\alpha = 0.707\,(3A - 1). \tag{4}$$

By substituting (1), (2), and (4) into (3), the formula for calculating the excess pore water pressure in the soil around the pile can be obtained:

$$\begin{aligned}\text{in the plastic zone } &\frac{\Delta u}{C_u} = 2\ln\left(\frac{R_p}{r}\right) + 1.73A - 0.58,\\ \text{in the elastic zone } &\frac{\Delta u}{C_u} = 0.578\,(3A - 1)\left(\frac{R_p}{r}\right)^2,\\ \text{on the surface of the pile } &\frac{\Delta u_{\max}}{C_u} = \ln\left[\frac{E}{2\,(1+\mu)C_u}\right] + 1.73A - 0.58,\\ \text{the radius of the plastic zone is } &\frac{R_p}{r_0} = \sqrt{\frac{E}{2\,(1+\mu)C_u}},\end{aligned} \tag{5}$$

where E is the elastic modulus of soil, μ is Poisson's ratio of soil, and R_0 is the pile radius.

3. Test Scheme

3.1. Model Box and Preparation of Foundation. The model test was carried out in a large-scale model box in the Qingdao University of Technology laboratory (Figure 1).

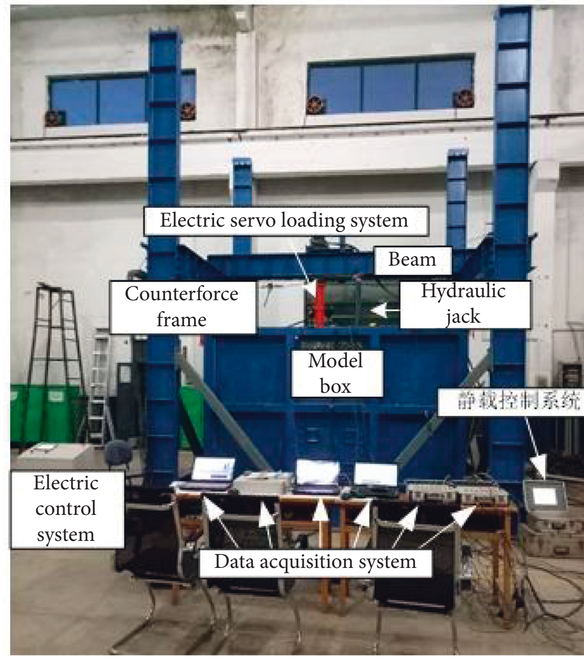

Figure 1: Large model test device.

The large-scale model's length × width × height is 2800 mm × 2800 mm × 2000 mm, and the model is placed on a base measuring 4 000 mm × 4 000 mm (length × width). The viscous soil used in the test comes from a silty clay layer, and the field soil samples are dried, crushed, screened, and sprayed with water to consolidate the soil [31]. The basic physical indexes of foundation soil after preparation are shown in Table 1.

3.2. Test Piles. In this paper, 2 test piles, TP1 and TP2, were tested using the indoor model test. The model pile was designed using aluminum material, with an elastic modulus of 72 GPa and Poisson's ratio of 0.3. According to similarity theory, the length of model piles TP1 and TP2 is 1000 mm, the outer diameter is 140 mm, and the inner diameter is 100 mm. Closed-end model pile TP1 is a single-wall model pipe pile with round pipe, and the pile end was installed using a flat plate with the same diameter as the pile. In order to effectively monitor the soil plug resistance on the inner wall of the pile, a double-wall open-end pipe pile TP2 was developed. A 20 mm gap was created between the inner and outer piper to create installation space for the microsensor and avoid damage to the sensor by soil entering into the pile.

3.3. Sensor Layout. In order to obtain the earth pressure and pore water pressure at the pile-soil interface, a silicon piezoresistive sensor was embedded in the model pile (Figure 2) [32]. The sensor range is specially customized according to the model experiments' earth pressure value, and the smaller the sensor's range, the smaller the sensor size. The earth pressure sensor and pore water pressure sensor surface are completely flush with the model pile surface. A silicon piezoresistive earth pressure sensor and pore water pressure

Table 1: Physical and mechanical parameters of foundation soil.

Soil classification	Relative density ds	Unit weight γ/(kN/cm^3)	Moisture content w (%)	Liquid limit w_L (%)	Plastic limit w_P (%)	Plasticity index I_p (%)	Cohesion c (kPa)	Internal friction angle φ/(o)	Compression modulus $E_{s1\text{-}2}$ (MPa)
Clay soil	2.73	18.0	35	35	21.2	13.5	14.4	8.6	3.3

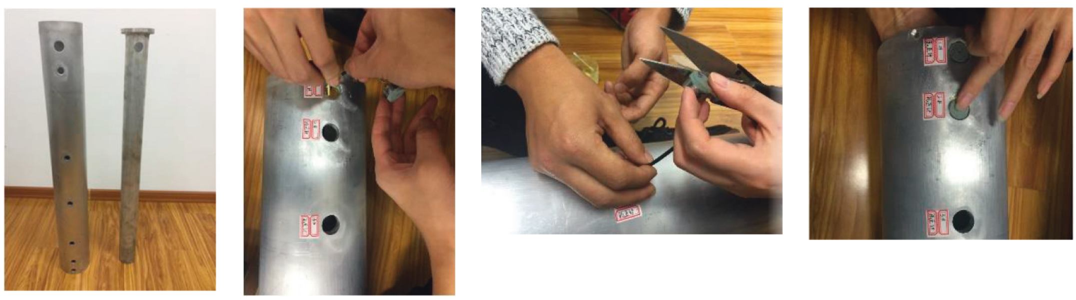

(a) (b) (c) (d)

Figure 2: Images showing the sensor installation process (unit: mm): (a) opening, (b) applying glue, (c) protection, and (d) installation.

sensor are installed on the same horizontal section using the same installation method. Six soil pressure and pore water pressure sensors were installed at unequal distances on the surface of the model pile, with a spacing of 50 mm, 100 mm, 200 mm, 200 mm, and 300 mm, respectively. The sensors were numbered 1#~6# from the pile end to the pile top, corresponding to $h/L = 1/20$, 1/10, 1/5, 2/5, 3/5, and 9/10 (h is the height between the sensor and pile end; L is the length of model pile). The force of the pile body near the pile end is significantly greater than the upper part of the pile body during pile jacking, and the closer it is to the pile end, the more obvious the effective radial stress degradation of the pile-soil interface is. Installing sensors at unequal distances on the surface of the model pile is beneficial to studying the length effect of the pile and the effective radial stress degradation of the pile interface caused by the length effect, which is conducive to accurately estimating the pile side friction resistance.

By placing temperature self-compensated fiber Bragg grating earth pressure sensor on the pile top loading platform, the change in pile jacking resistance can be obtained. A FS2200RM demodulator was used to automatically collect and save the FBG sensor data during the pile jacking process. The earth pressure and pore water pressure at the pile-soil interface were collected in real time using a CF3820 high-speed static signal test analyzer.

3.4. Experimental Scheme. The open and closed two pile types are sinking in the same test conditions. One time load is performed during the pile sinking process, the pile sinking speed is 300 mm/min, and the pile sinking depth is 900 mm. The soil layer of this test is homogeneous. To make the most of the test conditions, the open and closed piles are pressed into the soil in the middle of the model box. In this paper, through the development of open model piles and closed model piles with interface sensors, the indoor test of jacked sinking piles in open piles and closed piles in clay soil was carried out, and the changes in excess pore pressure and earth pressure of the pile-soil interface were studied.

4. Pile Jacking Test Results and Analysis

4.1. Pile Jacking Pressure during Pile Jacking. The pile jacking pressure was measured according to the total wavelength difference and the temperature wavelength difference during the pile jacking process using a temperature self-compensation pressure sensor. The pile jacking pressure formula is as follows [33]:

$$F = \frac{\Delta\lambda_B}{K_\varepsilon} A_p, \tag{6}$$

where F is pile jacking pressure, kN, $\Delta\lambda_B$ is the wavelength difference, nm, K_ε is the sensitivity coefficient, nm/MPa, and A_p is the cross-sectional area of the pile, m^2.

The change curve of pile jacking pressure with penetration depth during pile jacking is shown in Figure 3. TP1 and TP2 pile jacking pressure varies with penetration depth in a similar way, but TP1 has a larger pile jacking pressure, and the pile jacking pressure of TP1 is 15.8% greater than that in TP2 at the end of pile jacking because test pile TP2 is an open-end pipe pile, which forms a soil plug during the pile jacking process. The actual soil plug height of the model pile was small and the soil plug height was 329 mm when the burial depth was 900 mm. As a result, the pile jacking resistance and pile jacking pressure will be small. With continuous penetration of the pile into the soil, the stress state of the open-end pile gradually becomes similar to that of the closed-end pipe pile. The open pile is converted from a shallow partial occlusion that penetrates into the initial stage to a soil plug and will produce a plug effect; as the pile body penetrates, the earth plug is inside the pipe pile. The walls generate increasing friction until they are close to the degree

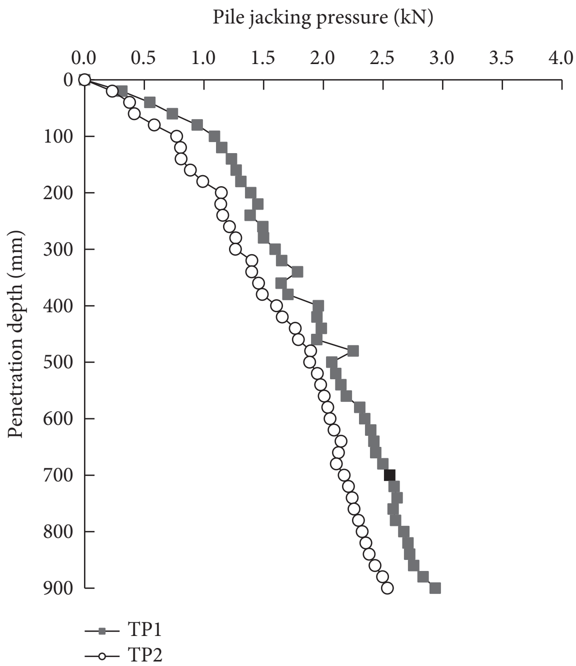

Figure 3: Pile driving pressure for open-end and closed-end piles.

of complete occlusion, presenting the sinking characteristics of closed piles.

4.2. Analysis of Excess Pore Water Pressure at Pile-Soil Interface. Pore water pressure is directly measured using a silicon piezoresistive pore water pressure sensor. The excess pore water pressure is the difference between the measured total pore water pressure and the hydrostatic pressure. The hydrostatic pressure is constant, and the change is the excess water pressure during pile jacking process and static load test process:

$$u_c = u - u_a, \tag{7}$$

where u_c is the excess pore water pressure, kPa, u is the total pore water pressure, kPa, and u_a is hydrostatic pressure, kPa.

With the increase of the depth of soil entry, the pressure of the soil covered around the pile increases, the extrusion and shearing effect of the soil around the pile become more and more intense, and the squeezing effect on the deep soil during the pile sinking process is more obvious. Under different penetration depths, the excess pore water pressure gradually increases with increasing depth, and the increasing trend is approximately a straight line at first followed by a sudden increase (Figure 4, the numbers of the legend in Figure 4 represent the penetration depths). During the pile jacking process, due to the continuous disturbance and compression of soft soil, too much pore water pressure is easily generated while the soil at the pile end suffers the greatest disturbance, so the excess pore water pressure at the pile end increases faster with increasing depth. At the same depth, excess pore water pressure decreases with increasing penetration depth because the amount of friction increases with increasing penetration depth, the soil is constantly disturbed, and the radial earth pressure on the pile side is gradually released, leading to a decrease in excess pore water pressure with increasing penetration depth at a certain depth.

By comparing the variation trend of excess pore water pressure between TP1 and TP2, it can be found that, with increasing depth, excess pore water pressure for test pile TP1 is generated faster because test pile TP1 is a closed-end pile, which has a significant soil squeezing effect in the pile jacking process and has a greater soil disturbance and radial deformation. As a result, the excess pore water pressure of test pile TP1 increases faster. As pile TP1 has a more significant soil squeezing effect than TP2, the excess pore water pressure for test pile TP1 is 1.04~1.24 times that of TP2.

4.3. Analysis of Earth Pressure at the Pile-Soil Interface. The change law of earth pressure at the pile-soil interface of the two test piles is consistent with the penetration depth (Figure 5). The deformation in the pile sinking process cannot be fully recovered after a certain time after the end of the pile, the radial effect force still exists, and the deformation during the loading process is superimposed on the deformation of the pile. Lateral earth pressure increases rapidly near the pile end with increasing depth because the area near the pile end has the greatest soil disturbance and produces the strongest compaction effect, and there is a compaction zone at the pile end, within which the overburden soil is heavy and the actual contact area of the pile soil is the largest, leading to a maximum earth pressure at the pile-soil interface and the fastest growth rate. At the same depth, the earth pressure at the pile-soil interface decreases with increasing penetration depth because at this depth, with increasing penetration depth, the amount of friction increases gradually, and there is a mud film between the pile and soil, which releases the earth pressure at the pile-soil interface. Therefore, the earth pressure at the pile-soil interface at the same depth decreases with increasing depth.

Compared with pile TP2, the earth pressure at the pile-soil interface of pile TP1 was higher, and the maximum earth pressure was 13.1% higher than that of pile TP2 because test pile TP1 is a closed-end pile, and its compaction effect is more significant than that of the open-end pile TP2 with the same diameter (Figure 5). Pile TP1 also has a greater disturbance to the soil; therefore, the earth pressure at the pile-soil interface of the test pile TP1 is larger.

4.4. Analysis of Effective Earth Pressure at the Pile-Soil Interface. The effective earth pressure at the pile-soil interface can be calculated by the following formula:

$$\sigma' = \sigma - \mu_c, \tag{8}$$

where σ' is the effective earth pressure, kPa, σ is the total earth pressure, kPa, and μ_c is the excess pore water pressure, kPa.

The curve of the effective earth pressure at the pile-soil interface is similar to that at the pile-soil interface with varying earth pressure with depth (Figure 6). The effective

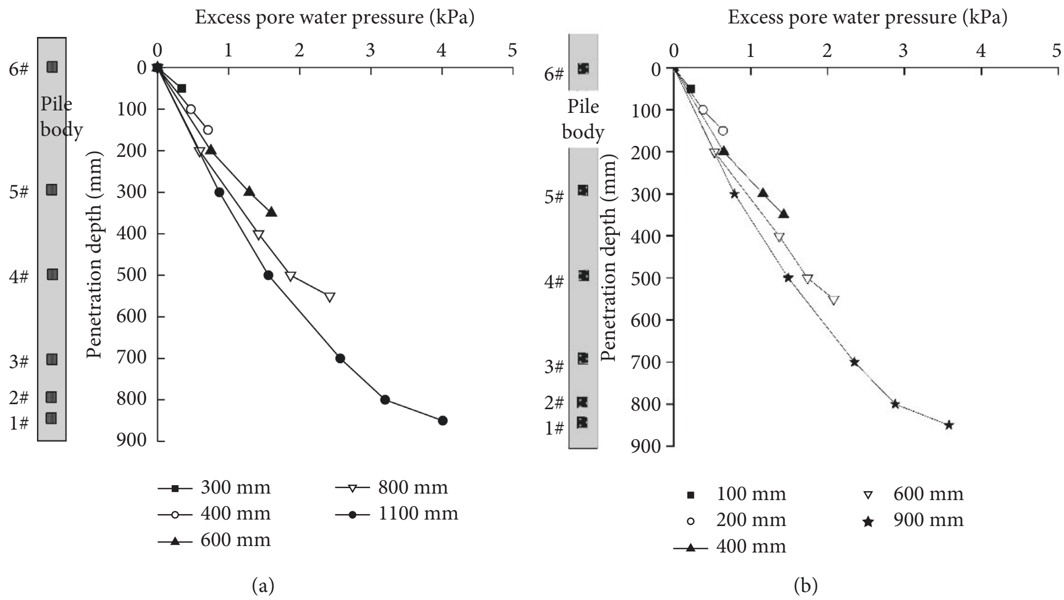

FIGURE 4: Excess pore water pressure distribution diagram for test piles TP1 and TP2 during the sinking process: (a) TP1, (b) TP2.

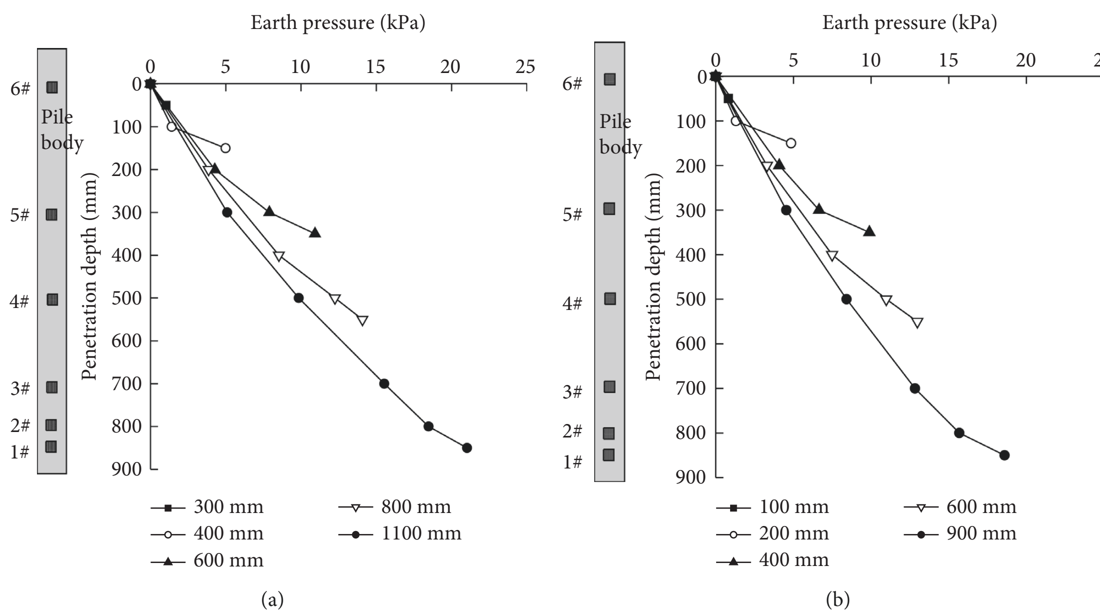

FIGURE 5: Distribution of earth pressure for test piles TP1 and TP2 during pile jacking: (a) TP1, (b) TP2.

earth pressure at the pile-soil interface increases gradually with increasing penetration depth and increases faster at the pile end due to the increased soil squeezing effect. At the same depth, the effective earth pressure at the pile-soil interface deteriorates. The effective earth pressure at the pile-soil interface is an important part of the earth pressure at the pile-soil interface. The degradation of effective earth pressure at the pile-soil interface is the main reason for the degradation of pile side friction. The experimental results further confirm that there is a degradation effect of pile side friction resistance at the same depth in the penetration process, and the relative distance of pile end h/D has a certain influence on pile side friction resistance, and when calculating pile side friction resistance, due to the friction resistance of the inner side of the open pile, it is necessary to consider the influence of the soil plug effect on the outer friction resistance of the pile.

Because the ratio between the excess pore water pressure and the earth pressure at the pile-soil interface is small, the effective earth pressure at the pile-soil interface of pile TP1 is also greater than that of pile TP2. Because pile TP1 is a closed-end pile, the effective earth pressure at the pile-soil interface of pile TP1 during the whole pile jacking process is 1.7%~23.7% higher than that of pile TP2.

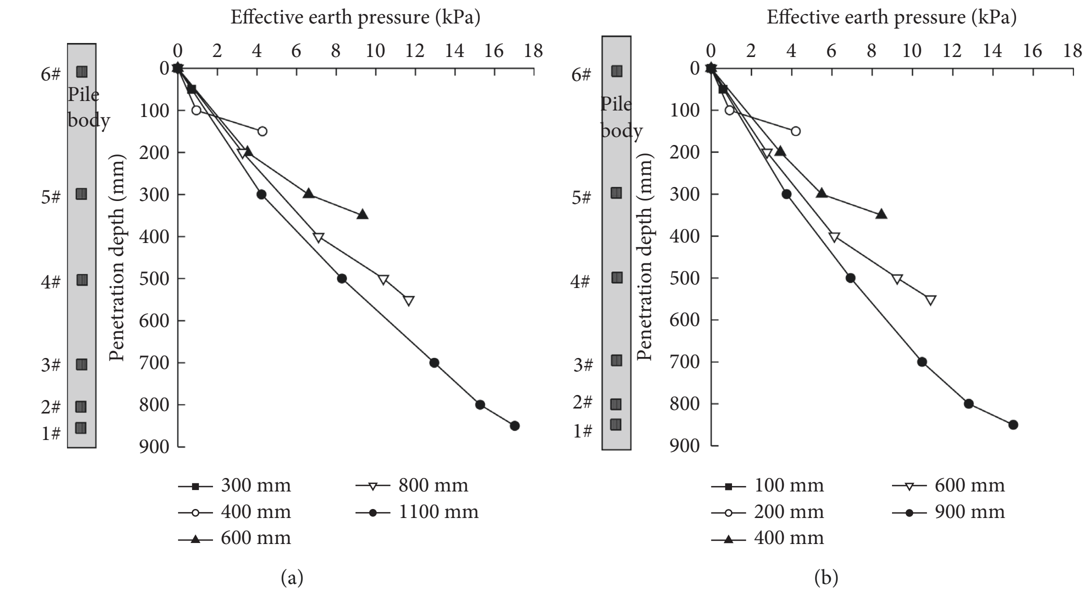

Figure 6: Distribution of effective earth pressure on test piles TP1 and TP2 during pile jacking: (a) TP1, (b) TP2.

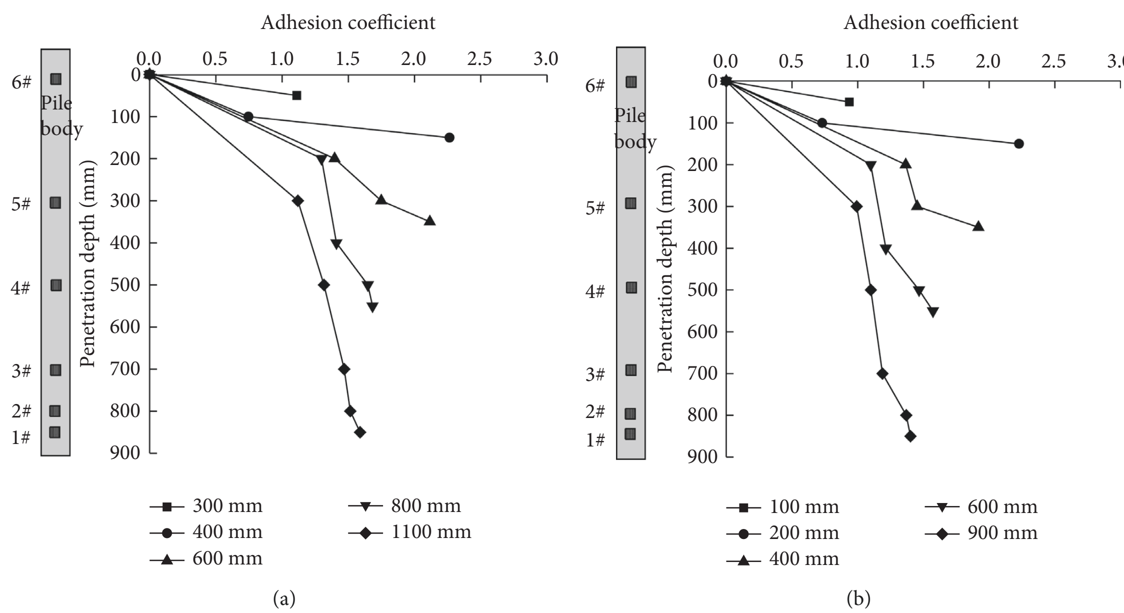

Figure 7: Change trend of adhesion coefficient of the pile-soil interface during pile jacking process: (a) TP1, (b) TP2.

4.5. Analysis of Pile-Soil Interface Adhesion Coefficient. The pile-soil interface adhesion coefficient represents the adhesion degree between the pile and soil; that is, the adhesion coefficient is equal to the ratio of effective earth pressure P' and horizontal deadweight stress σ_{cx} at the pile-soil interface. The adhesion coefficient t_c can be customized according to the following formula:

$$t_c = \frac{P'}{\sigma_{cx}}, \tag{9}$$

where when $t_c = 0$, the pile and soil is isolated. At $t_c > 1$, the effective earth pressure is greater than the original horizontal deadweight stress due to compaction.

The greater the effective earth pressure at the pile-soil interface, the greater the adhesion coefficient of the pile-soil interface and the higher the adhesion degree between the pile and soil, that is, the larger the actual contact area between pile and soil.

The adhesion coefficient at different pile depths increases with increasing penetration depth and is greater than 1 at greater depths because with increasing depth, the soil squeezing effect increases gradually, the effective earth pressure at the pile-soil interface increases at a faster speed, and the value is higher than the horizontal deadweight stress, and the higher amplitude increases with depth, so the adhesion coefficient of the pile-soil interface increases with

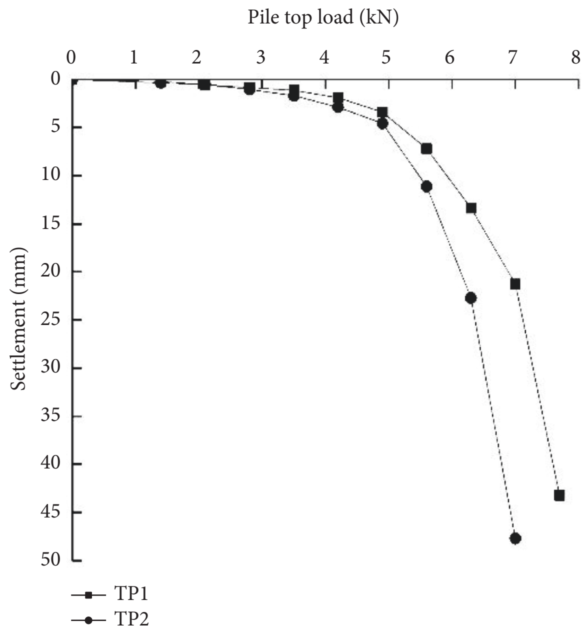

Figure 8: Q-s curve.

penetration depth (Figure 7). It further indicates that the higher the effective earth pressure at the pile-soil interface, the tighter the adhesion between pile and soil and the greater the actual contact area between pile and soil, which is manifested as a gradual increase in pile side resistance. At the same depth, the adhesion coefficient decreases gradually with increasing depth. The reasons are as follows: with increasing depth, the amount of shear and friction at the same depth increases, the pile side stress is gradually released, the effective earth pressure at the pile-soil interface decreases, and the adhesion coefficient of the pile-soil interface decreases with increasing depth. The degree of adhesion between piles and soil is weakened, indicating that the pile side resistance degrades along with the depth at the same depth.

5. Static Load Test Results and Analysis

5.1. Q-s Curve Analysis. Q-s curves can reflect load transfer behavior, pile-soil interactions, and pile failure mode; hence, analyzing Q-s curves is helpful for examining the vertical compressive bearing behavior of a single pile. The pile top settlement of test piles TP1 and TP2 changes with pile top load (Figure 8).

The Q-s curves of the two test piles show a steep drop (Figure 8). The curve is roughly divided into three stages: when the load is less than 3.5 kN, the curve is approximately straight line; when the load of test pile TP1 is greater than 3.5 kN and less than 6.3 kN, and the load of TP2 is greater than 3.5 kN and less than 5.6 kN, the curve entered the bending section; when the load of test pile TP1 is greater than 6.3 kN and TP2 is greater than 5.6 kN, the curve showed a steep drop. The soil around the pile will yield in the last two stages.

When the final load is applied, the pile top displacement values of test piles TP1 and TP2 are 43.24 mm and 47.72 mm, respectively, reaching the test end conditions specified in the code [26]. The ultimate bearing capacities of the two test piles in soft soil are 7.0 kN and 6.3 kN, respectively. After pile compression is completed, the pore water pressure in the soil beside the pile gradually dissipates over time, the soil reconsolidates, and the soil strength gradually recovers. The final pressures of test piles TP1 and TP2 are 2.94 kN and 2.54 kN, respectively. After 30 days of static load testing, the vertical bearing capacities of a single TP1 and TP2 pile were measured to be 2.38 and 2.48 times the final pressure, respectively. With the development of thixotropic recovery and consolidation aging, bearing capacity significantly increases. Compared with TP1, the final pressure and vertical bearing capacity of TP2 are smaller, but after the rest period, the development of bearing capacity is similar to TP1. The reason is that test pile TP2 is an open-end pile, which will produce soil plug in the process of pile jacking, and the soil plug is basically closed at the end of pile jacking. After the rest period, the soil plug and the pile wall are more closely bonded, and the soil around the pile is gradually consolidated and restored. It is more similar to the stress state of the closed-end pile, so the development of the bearing capacity is similar after the rest period.

5.2. Analysis of Results of Excess Pore Water Pressure at the Pile-Soil Interface. Under the action of various loads, the excess pore water pressure of pile TP2 increases gradually with increasing depth (Figure 9). The curve above 800 mm is steep; that is, the development of excess pore water pressure is slow with increasing depth. The curve below 800 mm becomes shallower; that is, the excess pore water pressure grows faster with increasing depth because in the process of static loading, the pile and soil undergo relative displacement and soil disturbance increase near the pile end, resulting in a rapid increase in excess pore water pressure at the pile end. With increasing load at the same depth, the excess pore water pressure at the pile-soil interface increases gradually. With increasing pile top load, the relative displacement between pile and soil increases, the soil compaction degree increases, and the excess pore water pressure at the pile-soil interface increases.

Compared with the value of the excess pore water pressure generated in the pile jacking process and under static load, the excess pore water pressure generated under static load is smaller. When the pile top load is 7.0 kN, the maximum excess pore water pressure at the pile end is 1.46 kPa, which is only 40.8% of the excess pore water pressure generated during pile jacking. The relative displacement between the pile and soil is small during static loading, the disturbance degree is small, and the compaction degree of soil is also small. In the pile jacking process, soil is continuously expelled outward, which causes significance disturbance to the soil, and the excess pore water pressure generated during pile jacking is large.

5.3. Analysis of Earth Pressure at the Pile-Soil Interface. Under the pile top load at all levels, the earth pressure at pile-soil interface increases in a straight line with increasing

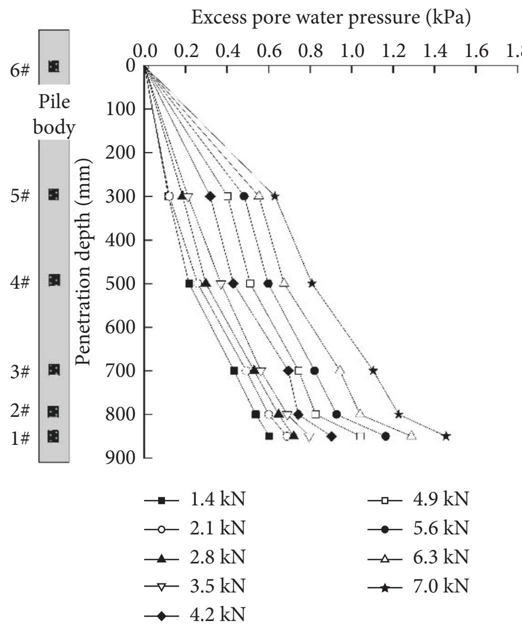

Figure 9: Change in excess pore water pressure of test pile TP2 with depth under various loads.

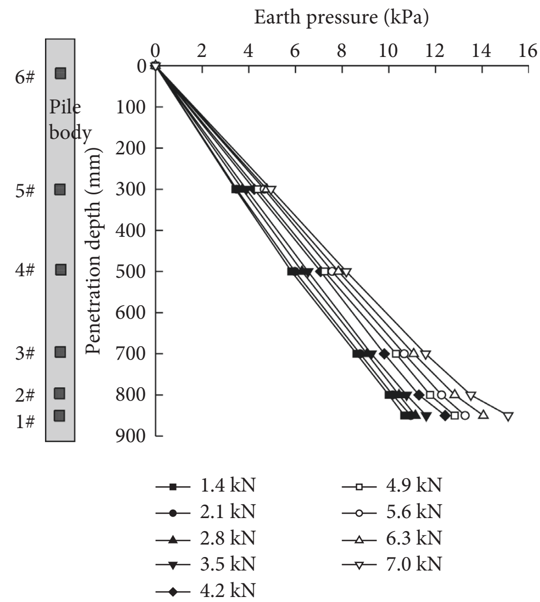

Figure 10: Variation of earth pressure at the pile-soil interface of TP2 with depth under various loads.

depth (Figure 10). The overburden soil weight increases with increasing depth, which makes the earth pressure at the pile-soil interface increase gradually. At the same depth, the earth pressure at the pile-soil interface gradually increases with increasing pile top load, and the increasing amplitude also shows a gradual increasing trend. With increasing pile top load, the pile top settlement increases, and the radial earth pressure increases with the soil compaction degree increasing.

Compared with the earth pressure at the pile-soil interface in the pile jacking process, the earth pressure at the pile-soil interface in the process of static load is smaller because the pile jacking mechanism is different from that of static loading. Pile jacking is a dynamic process, in which the soil around the pile is continuously displaced, the soil squeezing effect is strong, the generated earth pressure at the pile-soil interface is large, and the earth pressure "degrades" with increasing penetration depth at the same depth. In the static loading process, the pile top settlement is relatively small. Due to the small compaction degree of the pile top settlement relative to the surrounding soil, the earth pressure at the pile-soil interface is relatively small. In the static load process, the duration of each loading stage is relatively long, and the strength of disturbed soil gradually recovers.

5.4. Analysis of Effective Earth Pressure at the Pile-Soil Interface. The effective earth pressure at the pile-soil interface is similar to the change curve of earth pressure in Figure 10 (Figure 11). The effective earth pressure at the pile-soil interface increases gradually with increasing depth and increases approximately in a straight line. The effective earth pressure is the difference between the earth pressure and the excess pore water pressure, which only accounts for 3.4%~12.7% of the earth pressure and plays a small role. Therefore,

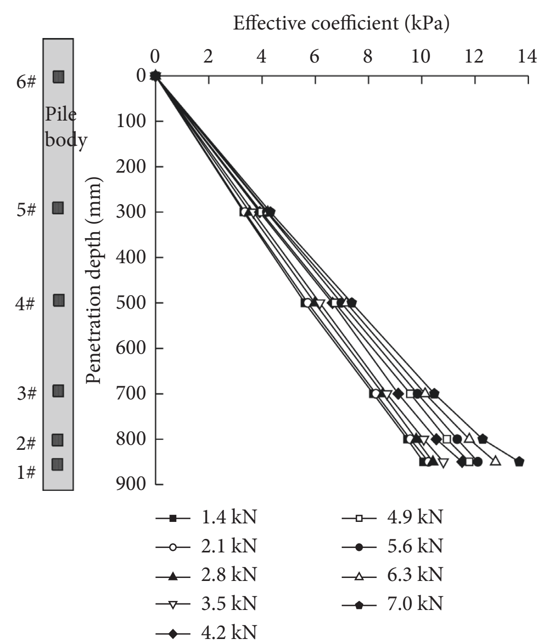

Figure 11: Variation curve of effective earth pressure of TP2 with depth under various loads.

the variation trend of the effective earth pressure at the pile-soil interface is similar to that of the earth pressure. With increasing pile top load, the amplitude of effective earth pressure gradually increases, and the closer it is to the pile end, the larger the amplitude increase is: the maximum is 0.0274 kPa/mm. With increasing pile top load, the compaction effect of the pile on soil increases gradually, and the closer it is to the pile end, the stronger the compaction effect becomes. In addition, compared with the pile jacking process, due to the longer load holding time in the static loading process, the pile body settlement is smaller, the soil

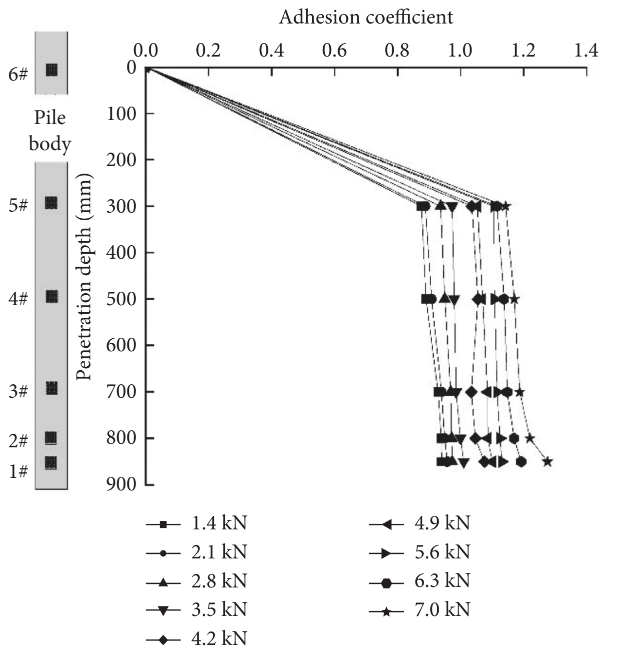

Figure 12: Variation curve of TP2 adhesion coefficient with depth under various loads.

squeezing effect is weaker, and the effective earth pressure on the side of the pile is also smaller. The adhesion coefficient values in this paper are slightly less than the values based on Meyerhof failure mode of ultimate bearing capacity.

5.5. Analysis of Adhesion Coefficient of the Pile-Soil Interface. Under the action of various loads, adhesion coefficient increases gradually with increasing depth, and when the pile top load is small, the pile side resistance shows a trend of large up and small down (Figure 12). Under the action of pile top load, pile settlement occurs, and with increasing depth, the actual contact area between pile and soil increases, resulting in a gradual increase of adhesion coefficient with the depth. The pile side resistance is gradually exerted from top to end, and the pile side resistance caused by the lower soil layer is less when the load is small. With increasing pile top load, the pile side resistance of the upper soil layer is gradually fully exerted, while that of the lower soil layer begins exerting. Under the action of maximum pile top load, the pile side resistance always increases with depth.

At the same depth, with increasing pile top load, adhesion coefficient increases gradually, indicating that the adhesion degree between piles and soil increases gradually. With increasing pile top load, the pile top settlement gradually increases and the earth pressure at the pile-soil interface increases, which results in increasing the actual contact area between the pile and soil, increasing the adhesion degree between the pile and soil and showing that the pile side resistance increases with increasing pile top load at the same depth. Numerically, the adhesion coefficient at the position of the #1 to #5 sensors ranges within 0.875–1.275, which is approximately 1, indicating that the earth pressure in the static loading process is approximately the static earth pressure.

6. Conclusion

In this paper, through large-scale indoor model tests of open- and closed-end pile jacking in saturated viscous soil, the change rules of effective earth pressure and adhesion coefficient at the pile-soil interface during pile jacking and static load test are examined, and the following conclusions are drawn:

(1) Under different pile depths, the excess pore water pressure, earth pressure, and effective earth pressure at the pile-soil interface of the open- and closed-end pile increase gradually with penetration depth, and the increase trend is approximately a straight line at first, followed by a sudden increase at the pile end. The soil squeezing effect of the closed-end pile is more significant than that of the open-end pile. The excess pore water pressure for closed-end pile is 1.04~1.24 times the open-end pile. The maximum earth pressure at the pile-soil interface of closed-end pile was 13.1% higher than that of open-end pile. At the same penetration depth, the excess pore water pressure, earth pressure, and effective earth pressure decrease with increasing penetration depth; that is, there is a "side pressure degradation" phenomenon, and the "degradation" phenomenon of open- and closed-end pile is consistent.

(2) The excess pore water pressure and effective earth pressure of the pile-soil interface gradually increase with the depth increasing during the pile sinking process. The incremental amplitude is related to the different h/D positions of the pile body at the end of the pile sinking. The increment amplitude decreases as h/D increases. The incremental amplitude of the closed-end pile at the same h/D position is greater than that of the open-end pile.

(3) Compared with the excess pore water pressure, the earth pressure and effective earth pressure generated during pile jacking and the force generated during static loading are relatively small. The maximum excess pore water pressure at the pile end is only 40.8% of the excess pore water pressure generated during pile jacking. Earth pressure does not "degrade" during static loading.

(4) In static load test, adhesion coefficient increases with increasing depth. At the same depth, with increasing pile top load, adhesion coefficient and adhesion degree of the pile-soil interface gradually increase.

Data Availability

The data used to support the findings of this study are available from the corresponding author upon request.

Conflicts of Interest

The authors declare that they have no conflicts of interest.

Acknowledgments

This research was supported by the National Key Research and Development Plan (2021YFE0113400).

References

[1] J. Yang, L. G. Tham, P. K. K. Lee, and S. T. F. Chan, "Behaviour of jacked and driven piles in sandy soil," *Géotechnique*, vol. 56, no. 4, pp. 245–259, 2006.

[2] Z. Wang, L. Miao, and F. Wang, "Theoretical and numerical analysis of jacked pile in sand," in *Proceedings of the Geo Congress 2012: State of the Art and Practice in Geotechnical Engineering*, pp. 245–254, Oakland, CA, USA, 2012.

[3] L. Li, J. Li, D. A. Sun, and L. Zhang, "Time-dependent bearing capacity of a jacked pile: an analytical approach based on effective stress method," *Ocean Engineering*, vol. 143, pp. 177–185, 2017.

[4] L. M. Zhang and H. Wang, "Field study of construction effects in jacked and driven steel H-piles," *Géotechnique*, vol. 59, no. 1, pp. 63–69, 2009.

[5] S. Yan, Z. Jia, W. Liu, and J. Li, "Research on the large diameter and supper long pile running under self-weight in the ocean engineering," *Journal of Coastal Research*, vol. 73, no. sp1, pp. 809–814, 2015.

[6] D. Chaney, K. Demars, and J. H. Chin, "Tests on model jacked piles in calcareous sand," *Geotechnical Testing Journal*, vol. 19, no. 2, p. 164, 1996.

[7] W. Lee, W.-J. Lee, S.-B. Lee, and R. Salgado, "Measurement of pile load transfer using the Fiber Bragg Grating sensor system," *Canadian Geotechnical Journal*, vol. 41, no. 6, pp. 1222–1232, 2004.

[8] G.-W. Li, H.-F. Pei, J.-H. Yin, X.-C. Lu, and J. Teng, "Monitoring and analysis of PHC pipe piles under hydraulic jacking using FBG sensing technology," *Measurement*, vol. 49, pp. 358–367, 2014.

[9] J. P. Cater, M. F. Randolph, and C. P. Wroth, "Stress and pore pressure changes in clay during and after the expansion of a cylindrical cavity," *International Journal for Numerical and Analytical Methods in Geomechanics*, vol. 3, no. 4, pp. 305–322, 1979.

[10] S.-L. Shen, J. Han, H.-H. Zhu, and Z.-S. Hong, "Evaluation of a dike damaged by pile driving in soft clay," *Journal of Performance of Constructed Facilities*, vol. 19, no. 4, pp. 300–307, 2005.

[11] L. F. Cao, C. I. Teh, and M. F. Chang, "Undrained cavity expansion in modified Cam clay I: theoretical analysis," *Géotechnique*, vol. 51, no. 4, pp. 323–334, 2001.

[12] F. S. Tehrani, F. Han, R. Salgado, M. Prezzi, R. D. Tovar, and A. G. Castro, "Effect of surface roughness on the shaft resistance of non-displacement piles embedded in sand," *Géotechnique*, vol. 66, no. 5, pp. 1–15, 2016.

[13] S. E. Burns and P. W. Mayne, "Pore pressure dissipation behavior surrounding driven piles and cone penetrometers," *Transportation Research Record: Journal of the Transportation Research Board*, vol. 1675, no. 1, pp. 17–23, 1999.

[14] C. Sagaseta, "Analysis of undrained soil deformation due to ground loss," *Géotechnique*, vol. 37, no. 3, pp. 301–320, 1987.

[15] L. T. Hoang, K. X. Dao, X. Xiong, and T. Matsumoto, "Performance analysis of a jacked-in single pile and pile group in saturated clay ground," *Soils and Foundations*, vol. 62, no. 1, Article ID 101094, 2022.

[16] J. Xue, A. Aloisio, Y. Lin, M. Fragiacomo, and B. Briseghella, "Optimum design of piles with pre-hole filled with high-damping material: experimental tests and analytical modeling," *Soil Dynamics and Earthquake Engineering*, vol. 151, Article ID 106995, 2021.

[17] J.-H. Hwang, N. Liang, and C. H. Chen, "Ground response during pile driving," *Journal of Geotechnical and Geoenvironmental Engineering*, vol. 127, no. 11, pp. 939–949, 2001.

[18] R. W. Cooke and G. Price, "Strains and displacements around friction piles," in *Proceedings of the 8th International Conference on Soil Mechanics and Foundation Engineering*, pp. 53–60, Moscow, 1973.

[19] J. M. Pestana, C. E. Hunt, and J. D. Bray, "Soil deformation and excess pore pressure field around a closed-ended pile," *Journal of Geotechnical and Geoenvironmental Engineering*, vol. 128, no. 1, pp. 1–12, 2002.

[20] P. Doherty and K. Gavin, "Shaft capacity of open-ended piles in clay," *Journal of Geotechnical and Geoenvironmental Engineering*, vol. 137, no. 11, pp. 1090–1102, 2011.

[21] B. M. Lenane, *Experimental Investigations of Pile Behaviour Using Instrumental Field piles [Dissertation]*, University of London (Imperial College), London, 1992.

[22] A. J. Bond and R. J. Jardine, "Shaft capacity of displacement piles in a high OCR clay," *Géotechnique*, vol. 45, no. 1, pp. 3–23, 1995.

[23] H. L. Kou, M. Y. Zhang, and F. Yu, "Shear zone around jacked piles in clay," *Journal of Performance of Constructed Facilities*, vol. 29, no. 6, Article ID 04014169, 2015.

[24] J. W. Liu, Z. M. Zhang, F. Yu, and Z.-Z. Xie, "Case history of installing instrumented jacked open-ended piles," *Journal of Geotechnical and Geoenvironmental Engineering*, vol. 138, no. 7, pp. 810–820, 2012.

[25] M. Y. Fattah, B. S. Zbar, and F. S. Mustafa, "Effect of soil saturation on load transfer in a pile excited by pure vertical vibration," *Proceedings of the Institution of Civil Engineers - Structures and Buildings*, vol. 174, no. 2, pp. 132–144, 2021.

[26] Y.-Y. Wang, S.-K. Sang, M.-Y. Zhang, D.-S. Jeng, B.-X. Yuan, and Z.-X. Chen, "Laboratory study on pile jacking resistance of jacked pile," *Soil Dynamics and Earthquake Engineering*, vol. 154, Article ID 107070, 2022.

[27] M. Y. Fattah and W. H. S. Al-Soudani, "Bearing capacity of closed and open ended pipe piles installed in loose sand with emphasis on soil plug," *Indian Journal of Geo-Marine Sciences*, vol. 45, no. 5, pp. 703–724, 2016.

[28] A. J. Abbo and S. W. Sloan, "A smooth hyperbolic approximation to the Mohr-Coulomb yield criterion," *Computers & Structures*, vol. 54, no. 3, pp. 427–441, 1995.

[29] Y.-Q. Tang, Z.-D. Cui, X. Zhang, and S.-K. Zhao, "Dynamic response and pore pressure model of the saturated soft clay around the tunnel under vibration loading of Shanghai subway," *Engineering Geology*, vol. 98, no. 3-4, pp. 126–132, 2008.

[30] R. M. Buckley, R. J. Jardine, S. Kontoe, and B. M. Lehane, "Effective stress regime around a jacked steel pile during installation ageing and load testing in chalk," *Canadian Geotechnical Journal*, vol. 55, no. 11, pp. 1577–1591, 2018.

[31] “The national standards compilation group of people’s Republic of China,” *GB/T50123-1999 Standard for Soil Test Method*, China Planning Press, Beijing, 1999.

[32] Y. Wang, X. Liu, M. Zhang, and S. S. Yang, “Field test of excess pore water pressure at pile-soil interface caused by PHC pipe pile penetration based on silicon piezoresistive sensor,” *Sensors*, vol. 20, no. 10, Article ID 2829, 2020.

[33] M. Yegian and G. Wrights, “Lateral soil resistance displacement relationships for pile fundation in soft clays,” in *Proceedings of the Offshore Technology Conference*, Houston, Texas, April 1973.